Published in final edited form as:

SIAM J Imaging Sci. 2022 ; 15(3): 1213–1228. doi:10.1137/21m1463409.

Analysis for Full-Field Photoacoustic Tomography with Variable Sound Speed

Linh Nguyen[†], **Markus Haltmeier**[‡], **Richard Kowar**[§], **Ngoc Do**[¶]

[†]Department of Mathematics, University of Idaho, 875 Perimeter Dr, Moscow, ID 83844, USA

[‡]Department of Mathematics, University of Innsbruck, Technikerstrasse 13, 6020 Innsbruck, Austria

[§]Department of Mathematics, University of Innsbruck, Technikerstrasse 13, 6020 Innsbruck, Austria

[¶]Department of Mathematics, Missouri State University, Springfield, Missouri, USA

Abstract

Photoacoustic tomography (PAT) is a non-invasive imaging modality that requires recovering the initial data of the wave equation from certain measurements of the solution outside the object. In the standard PAT measurement setup, the used data consist of time-dependent signals measured on an observation surface. In contrast, the measured data from the recently invented full-field detection technique provide the solution of the wave equation on a spatial domain at a single instant in time. While reconstruction using classical PAT data has been extensively studied, not much is known for the full field PAT problem. In this paper, we build mathematical foundations of the latter problem for variable sound speed and settle its uniqueness and stability. Moreover, we introduce an exact inversion method using time-reversal and study its convergence. Our results demonstrate the suitability of both the full field approach and the proposed time-reversal technique for high resolution photoacoustic imaging.

Keywords

full field; photoacoustic tomography; time reversal; uniqueness; stability; Neumann series

AMS subject classifications.

35R30; 35L05; 92C55

1. Introduction.

Consider the following initial value problem for wave equation for an inhomogeneous isotropic medium

lnguyen@uidaho.edu.

$$\begin{cases} \partial_t^2 p(x,t) - c^2(x)\Delta p(x,t) = 0 & \text{for } (x,t) \in \mathbb{R}^n \times (0,\infty) \\ p(x,0) = f(x) & \text{for } x \in \mathbb{R}^n \\ \partial_t p(x,0) = 0 & \text{for } x \in \mathbb{R}^n . \end{cases} \tag{1.1}$$

Here $c \in C^\infty(\mathbb{R}^n)$ denotes the sound speed and $f \in H_0^1(\mathbb{R}^n)$ the initial data that is supported inside a bounded domain $\Omega \subseteq \mathbb{R}^n$ with Lipschitz boundary. We assume that the sound speed is positive everywhere and constant on the complement $\Omega^c := \mathbb{R}^n \setminus \Omega$ of Ω. After rescaling we assume $c|_{\Omega^c} = 1$. We refer to the solution $p: \mathbb{R}^n \times [0,\infty) \to \mathbb{R}$ of (1.1) as acoustic pressure field and f as the initial pressure.

Recall that $f: \Omega \to \mathbb{R}$ is an element of the Sobolev space $H^1(\Omega)$ if it is Lebesgue measurable and $\| f \|_{H^1(\Omega)}^2 := \int_\Omega |\nabla f(x)|^2 \, dx + \int_\Omega |f(x)|^2 \, dx$ is finite. Also, $H_0^1(\Omega)$ consists of all elements in $H^1(\Omega)$ that vanish on the boundary $\partial\Omega$. The space $H_0^1(\Omega)$ is equipped with the norm $\| f \|_{H_0^1(\Omega)} := \sqrt{\int_\Omega |\nabla f(x)|^2 \, dx}$, which is equivalent to $\| \cdot \|_{H^1(\Omega)}$ when restricted to $H_0^1(\Omega)$. We note that each $f \in H_0^1(\Omega)$ can be extended to a function of $H^1(\mathbb{R}^n)$ using the value zero on Ω^c, which is tacitly done in this paper.

Full field photoacoustic tomography.

The aim of photoacoustic tomography (PAT) is to recover the initial pressure from certain observations of the acoustic pressure field made outside of Ω. In standard PAT, the data is given by the restricted pressure $p|_{S\times[0,T]}$, where $S \subseteq \mathbb{R}^n$ is an $(n-1)$-dimensional observation surface [28, 38, 9, 20, 4, 19, 11, 30]. Opposed to that, in full field PAT introduced in [26, 27], the data provide the acoustic pressure only for a single and fixed time T but on an n-dimensional measurement domain.

To be more specific, for given $T > 0$, we define the following two operators

$$\mathbf{W}_T : H_0^1(\Omega) \to H^1(\mathbb{R}^n) : f \mapsto p(\cdot, T), \tag{1.2}$$

$$\mathbf{W}_{T,\Omega} : H_0^1(\Omega) \to H^1\left(\overline{\Omega}^c\right) : f \mapsto p(\cdot, T)|_{\overline{\Omega}^c}, \tag{1.3}$$

where p is the solution of (1.1). We refer to $\mathbf{W}_T$ as the complete single time wave transform and to $\mathbf{W}_{T,\Omega}$ as the exterior single time wave transform. Full field PAT provides approximations of $\mathbf{W}_{T,\Omega} f$, from which one aims to recover approximations to the initial pressure f. In [40] it is outlined how actual full field PAT data can be reduced to $\mathbf{W}_{T,\Omega} f$.

In this paper we prove uniqueness and stability of inverting $\mathbf{W}_{T,\Omega}$. We also propose a time-reversal technique to derive a Neumann series solution for the inversion.

Related work.

For the standard PAT problem there is a vast literature on various practical and theoretical aspects (see, for example, [38, 20, 4, 19, 11, 30]). In that context, the time-reversal method

has been studied intensively [9, 15, 32, 33]. However, to the best of our knowledge, the time-reversal method has not developed for PAT with full field data.

Only few works exist [27, 26, 40, 13] on the full field inversion problem. The work [27] considers constant speed of sound and the problem is reduced to the inversion of the Radon transform. The work [40] deals with non-constant speed and uses the standard Landweber iterative method. However, the article uses the data in the whole space, not the exterior data as we consider here. In the proceeding [13], variational regularization is used with exterior data. Neither uniqueness nor stability has been proven there. In the present article, for the first time, we prove uniqueness and stability for inverting $\mathbf{W}_{T,\Omega}$. Moreover, we propose and analyze an iterative time-reversal procedure for its inversion.

2. Uniqueness and stability.

Let $\mathbb{R}^n$ be equipped with the metric $\mathbf{g} = c^{-2}(x)dx^2$. We denote by diam(Ω) the diameter of Ω, defined as the longest distance between any two points inside $\overline{\Omega}$ with respect to the metric $\mathbf{g}$. We recall that $T > 0$ is a fixed observation time and $\Omega \subseteq \mathbb{R}^n$ a bounded domain with Lipschitz boundary.

2.1. Uniqueness of reconstruction.

Our first aim is to prove the injectivity of $\mathbf{W}_{T,\Omega}$, which implies that the full field PAT problem is uniquely solvable. For that purpose we start by recalling a uniqueness result for the wave equation, obtained by Stefanov and Uhlmann [32].

Lemma 2.1. *Let* $f \in H_0^1(\mathbb{R}^n)$ *and suppose* $T > \frac{1}{2}\operatorname{diam}(\Omega)$. *If the solution* p *of* (1.1) *satisfies* $p(\cdot, T)|_{\Omega^c} = 0$ *and* $(\partial_t p)(\cdot, T)|_{\Omega^c} = 0$, *then* $f = 0$.

Denote by $B_R \subseteq \mathbb{R}^n$ the ball of radius $R > 0$ in the Euclidean metric of $\mathbb{R}^n$. We have the following result:

Lemma 2.2. *For* $\epsilon > 0$ *and* $h \in H_0^1(\mathbb{R}^n)$, *let* $u \in C([0, T], H^1(B_{T+\epsilon}))$ *satisfy*

$$\begin{cases} \partial_t^2 u(x,t) - \Delta u(x,t) = 0 & \text{for } (x,t) \in B_{T+\epsilon} \times [0,T] \\ u(x,0) = h(x) & \text{for } x \in B_{T+\epsilon} \\ \partial_t u(x,0) = 0 & \text{for } x \in B_{T+\epsilon}. \end{cases} \tag{2.1}$$

If $h(x) = 0$ *for* $x \in B_T$ *and* $u(x, T) = 0$ *for* $x \in B_\epsilon$, *then* $h(x) = 0$ *for* $x \in B_{T+\epsilon}$.

Proof. For u satisfying the Euler-Poisson-Darboux equation with initial data $(f, 0)$ instead of the wave equation (2.1), the result was proven in [2, 24]. The proof of the current situation is similar to [24, Theorem 2.1] and is therefore omitted. ■

In the following, for any $a > 0$, we write

$$\Omega_a^{(1)} := \left\{ x \in \mathbb{R}^n \mid \operatorname{dist}(x, \Omega) \le a \right\}$$

$$\Omega_a^{(2)} := \left\{ x \in \mathbb{R}^n \mid \operatorname{dist}(x, \Omega) \geq a \right\}.$$

Clearly, for $f \in H_0^1(\Omega)$ we have $\mathbf{W}_T f \in H_0^1\left(\Omega_T^{(1)}\right)$, due to finite speed of propagation.

Lemma 2.3. *Let* Ω *be convex,* $h \in H_0^1\left(\mathbb{R}^n\right)$ *and suppose u satisfies*

$$\begin{cases} \partial_t^2 u(x,t) - \Delta u(x,t) = 0 & \text{for } (x,t) \in \Omega^c \times [0,T] \\ u(x,0) = h(x) & \text{for } x \in \Omega^c \\ \partial_t u(x,0) = 0 & \text{for } x \in \Omega^c. \end{cases}$$

Then $u(x, T) = 0$ *for all* $x \in \Omega_T^{(2)}$ *implies* $h(x) = 0$ *for all* $x \in \Omega^c$.

Proof. Using Lemma 2.2, the proof follows the lines of [2, Proof of Theorem 3] and for the sake of brevity is omitted. ■

Here is our main uniqueness result.

Theorem 2.4 (Main injectivity result). *If* $T >$ diam(Ω)/2, *then the exterior single time wave transform* $\mathbf{W}_{T,\Omega}: H_0^1(\Omega) \to H^1\left(\overline{\Omega}^c\right)$ *is injective. In particular, the equation* $\mathbf{W}_{T,\Omega} f = g$ *has at most one solution in* $H_0^1(\Omega)$ *for* $g \in H^1\left(\overline{\Omega}^c\right)$.

Proof. Suppose $f \in H_0^1(\Omega)$ satisfies $\mathbf{W}_{T,\Omega} f = 0$ and denote by p the solution of (1.1). By definition we have $\mathbf{W}_{T,\Omega} f = p(\cdot, T)|_{\overline{\Omega}^c}$ and thus $p(x, T) = 0$ and $\Delta p(x, T) = 0$ for all $x \in \Omega^c$. Define $u(x, t) := \partial_t p(x, T - t)$. Then $\partial_t u(x,t) = -\partial_t^2 p(x, T-t) = -\Delta p(x, T-t)$ in Ω^c. Consequently,

$$\begin{cases} \partial_t^2 u(x,t) - \Delta u(x,t) = 0 & \text{for } (x,t) \in \Omega^c \times [0,T] \\ u(x,0) = \partial_t p(x,T) & \text{for } x \in \Omega^c \\ \partial_t u(x,0) = 0 & \text{for } x \in \Omega^c. \end{cases}$$

Because $u(x, T) = \partial_t p(x, 0) = 0$ in Ω^c, Lemma 2.3 shows $\partial_t p(x, T) = 0$ for all $x \in \Omega^c$. Now application of Lemma 2.1 gives $f = 0$. ■

2.2. Stability of inversion.

Let us first recall some microlocal analysis for the solution of the wave equation; see for example [32, 37] for more details. Let $\hat{f}(\xi) = \int_{\mathbb{R}^n} f(x) e^{-ix \cdot \xi}\, dx$ denote the Fourier transform of f. Let us for the moment assume that there are no two conjugate points within the distance T in $(\mathbb{R}^n, \mathbf{g})$. Then, up to infinitely smooth error, the solution p of (1.1) can be written as

$$p(x,t) = p^{+}(x,t) + p^{-}(x,t) \coloneqq \frac{1}{(2\pi)^n} \sum_{\sigma = \pm} \int_{\mathbb{R}^n} e^{i\phi_\sigma(x,\xi,t)} a_\sigma(x,\xi,t) \hat{f}(\xi) d\xi, \quad (x,t) \in \mathbb{R}^n \times [0,T]. \tag{2.2}$$

Here, the phase functions $\phi_\pm(x, \xi, t)$ are positively homogenous of order 1 in ξ and solve the eikonal equations

$$\begin{cases} \mp \partial_t \phi_\pm(x,\xi,t) = c(x) |\nabla_x \phi_\pm(x,\xi,t)| \\ \phi_\pm(x,\xi,0) = x \cdot \xi. \end{cases}$$

The functions $a_\pm$ are classical amplitudes of order 0 satisfying $a_\pm(x, \xi, 0) = 1/2$. The principal terms $a_\pm^{(0)}(x,\xi,t)$ satisfy $a_\pm^{(0)}(x,\xi,t) = 1/2$ and the homogenous equations

$$\left[(\partial_t \phi_\pm) \partial_t - c^2 \nabla \phi_\pm \cdot \nabla_x + C_\pm \right] a_\pm^{(0)} = 0, \tag{2.3}$$

where $C_\pm \coloneqq \left(\partial_t^2 - c^2 \Delta \right) \phi_\pm / 2$. Geometrically, each singularity $(x, \xi) \in \mathrm{WF}(f)$ is propagated by p_+ in the phase space along the positive bi-characteristic $(\gamma_{x,\xi}(t), \zeta_{x,\xi}(t))$, while propagated by p_- along the negative bicharacteristic given by $(\gamma_{x,-\xi}(t), \zeta_{x,-\xi}(t)) = (\gamma_{x,\xi}(-t), -\zeta_{x,\xi}(-t))$. Here, the bicharacteristic $(\gamma_{x,\xi}(t), \zeta_{x,\xi}(t)) = (x(t), \xi(t)) \in T^*\mathbb{R}^n$ is defined as the solution of

$$\begin{cases} \dot{x}(t) = \frac{\xi(t)}{|\xi(t)|_{\mathbf{g}}}, \quad x(0) = x, \\ \dot{\xi}(t) = -\frac{1}{2} \nabla \left(c^2(x(t)) \right) \left| \xi(t) \right|_{\mathbf{g}}, \quad \eta(0) = \xi, \end{cases}$$

where $|\xi|_{\mathbf{g}}$ is the length of ξ in the metric $\mathbf{g}$. Let us note that the projection $\gamma_{x,\xi}(t)$ of the bicharacteristic is a unit speed geodesic in $(\mathbb{R}^n, \mathbf{g})$. Its initial unit tangent vector is $\xi/|\xi|_{\mathbf{g}}$.

We consider the following so-called non-trapping condition.

Condition 2.5 (Non-trapping condition). *We assume that there exists $T_0 > 0$ such that there is no geodesic curve that intersects Ω with the length, in metric $\mathbf{g}$, bigger than T_0.*

It is worth noting that if Condition 2.5 holds then $\mathrm{diam}(\Omega) \leq T_0$.

For $h \in H^1(\mathbb{R}^n)$ consider the following time-reversed wave equation

$$\begin{cases} \partial_t^2 q(x,t) - c^2(x) \Delta q(x,t) = 0 & \text{for } (x,t) \in \mathbb{R}^n \times (0,T) \\ q(x,T) = h(x) & \text{for } x \in \mathbb{R}^n \\ \partial_t q(x,T) = 0 & \text{for } x \in \mathbb{R}^n. \end{cases} \tag{2.4}$$

We define the time-reversal operator

$$\mathbf{W}_T^\sharp : H^1(\mathbb{R}^n) \to H^1(\Omega) : h \to q(\cdot, 0)|_\Omega, \tag{2.5}$$

where q is the solution of (2.4). For a function $\Psi \in C_0^\infty(\mathbb{R}^n)$ denote by $\mathbf{\Psi}$ the pointwise multiplication operator $f \mapsto \Psi f$.

Proposition 2.6. *Let* $T > T_0/2$, *suppose* $\Psi \in C_0^\infty(\mathbb{R}^n)$ *and set* $x_\pm(x, \xi) := \gamma_{x,\xi}(\pm T)$. *Then* $\mathbf{W}_T^\sharp \mathbf{\Psi} \mathbf{W}_T : H_0^1(\Omega) \to H^1(\Omega)$ *is a pseudo-differential operator of order zero with principal symbol*

$$\sigma(x,\xi) = \frac{1}{4}[\Psi(x_+(x,\xi)) + \Psi(x_-(x,\xi))].$$

Proof. Our key idea is the construction of the parametrix of time-reversed wave equation (2.4), in the same spirit as [32, Proof of Theorem 3] but adapted to our context. From (2.2), up to smooth terms, we have $\mathbf{W}_T^\sharp \mathbf{\Psi} \mathbf{W}_T = \mathbf{W}_T^\sharp \mathbf{\Psi} \mathbf{W}_T^{(+)} + \mathbf{W}_T^\sharp \mathbf{\Psi} \mathbf{W}_T^{(-)}$ with

$$\mathbf{W}_T^{(\pm)} f(x) = p_\pm(x,T) = \frac{1}{(2\pi)^n} \int_{\mathbb{R}^n} e^{i\phi_\pm(x,\xi,T)} a_\pm(x,\xi,T) \hat{f}(\xi) d\xi .$$

It suffices to prove that $\mathbf{W}_T^\sharp \mathbf{\Psi} \mathbf{W}_T^{(+)}$ is a pseudo-differential operator with principal symbol $\sigma_+(x_0, \xi_0) = \Psi(x_+(x_0, \xi_0))/4$, for all $(x_0, \xi_0) \in T^*\Omega$.

Consider the parametrix of the time-reversed wave equation (2.4) with initial data $h = \mathbf{\Psi} \mathbf{W}_T^{(+)} f$, which can be written in the form

$$q_+(x,t) = \frac{1}{2(2\pi)^n} \int_{\mathbb{R}^n} e^{i\phi_+(x,\xi,t)} b(x,\xi,t) \hat{f}(\xi) d\xi + \frac{1}{2(2\pi)^n} \int_{\mathbb{R}^n} e^{i\phi_+(x,\xi,2T-t)} b(x,\xi,2T-t) \hat{f}(\xi) d\xi,$$

with $b(x, \xi, T) = \Psi(x) a_+(x, \xi, T)$. Let us note that the first summand in q_+ is a modification of the (positive) forward solution p_+ which in the case that $\Psi = 1$ exactly equals $p_+/2$. The second summand is the time-reflection of the first part through the value $t = T$. This construction imposes zero velocity at $t = T$. Indeed, it is easy to check that q_+ satisfies the initial conditions $q_+(x, T) = \mathbf{\Psi} \mathbf{W}_T^{(+)} f$ and $(q_+)_t(x, T) = 0$. Therefore, from the definition of $\mathbf{W}_T^\sharp$,

$$\begin{aligned} \mathbf{W}_T^\sharp \mathbf{\Psi} \mathbf{W}_T^{(+)} f = q_+(x,0) &= \frac{1}{2(2\pi)^n} \int_{\mathbb{R}^n} e^{i\phi_+(x,\xi,0)} b(x,\xi,0) \hat{f}(\xi) d\xi \\ &+ \frac{1}{2(2\pi)^n} \int_{\mathbb{R}^n} e^{i\phi_+(x,\xi,2T)} b(x,\xi,2T) \hat{f}(\xi) d\xi, \end{aligned} \tag{2.6}$$

up to infinitely smoothing terms.

Note that both the principal term $a_+^{(0)}(x, \xi, t)$ and $b^{(0)}(x, \xi, t)$ of $a_+(x, \xi, t)$ and $b(x, \xi, t)$, respectively, satisfy the homogeneous transport equation (2.3). Hence, their ratio on each bi-characteristic is constant. In particular,

$$\frac{b^{(0)}(x_0,\xi_0,0)}{a_+^{(0)}(x_0,\xi_0,0)} = \frac{b^{(0)}(x_+(x_0,\xi_0),\xi_+(x_0,\xi_0),T)}{a_+^{(0)}(x_+(x_0,\xi_0),\xi_+(x_0,\xi_0),T)} = \Psi(x_+(x_0,\xi_0)).$$

Let us consider (2.6). Since $\phi_+(0, x, \xi) = x \cdot \xi$, the first part on the right hand side is a pseudo-differential operator with principal symbol at (x_0, ξ_0) equals

$$\frac{1}{2}b^{(0)}(x_0, \xi_0, 0) = \frac{1}{2}a_+^{(0)}(x_0, \xi_0, 0)\Psi(x_+(x_0, \xi_0)) = \frac{1}{4}\Psi(x_+(x_0, \xi_0)).$$

The second summand of (2.6) is a Fourier integral operator that translates the singularity of f at $(\gamma_{x0,\xi_0}(-2T), \zeta_{x0,\xi_0}(-2T))$ to (x_0, ξ_0). From the condition $T > T_0/2$, we have $\gamma_{x0,\xi_0}(-2T) \in \Omega^c$. Therefore, $f = 0$ near $\gamma_{x0,\xi_0}(-2T)$, which implies the second part on the right hand side of (2.6) is infinitely smoothing. This concludes our proof. ■

Remark 2.7. Proposition 2.6 has been proven under the assumption that there are no two conjugate points within the distance T in $(\mathbb{R}^n, \mathbf{g})$. However, the proposition still holds when this condition fails. In that case, we split the time interval $[0, T]$ into subintervals such that on each subinterval the geodesic $\gamma_{x,\xi}(t)$ does not contain conjugate points. Applying above presented proof iteratively on each subinterval we derive Proposition 2.6 in the general case.

The following theorem provides the stability of solving the final time wave inversion problem.

Theorem 2.8 (Main stability result). *Assume that* $T > T_0/2$, *with* T_0 *as in Condition 2.5. Then, there exists a constant* $C = C(\Omega, T, c) > 0$ *such that*

$$\forall f \in H_0^1(\Omega): \quad \| f \|_{H_0^1(\Omega)} \leq C \| \mathbf{W}_{T,\Omega} f \|_{H^1(\overline{\Omega}^c)}. \tag{2.7}$$

Proof. Since $T > T_0/2$, there exists $a > 0$ such that for all $(x, \xi) \in T^*\Omega$ either $x_+(x, \xi) \in \Omega_a^{(2)}$ or $x_-(x, \xi) \in \Omega_a^{(2)}$. Let $0 \leq \Psi \in C_0^\infty(\mathbb{R}^n)$ be such that $\Psi \equiv 0$ on Ω and $\Psi \equiv 1$ on $\Omega_a^{(2)}$. Then $\mathbf{\Psi W}_{T,\Omega} = \mathbf{\Psi W}_T$ and thus Proposition 2.6 implies that $\mathbf{W}_T^\sharp \mathbf{\Psi W}_{T,\Omega}$ is a pseudo-differential operator with principal symbol $(\Psi(x_+(x, \xi)) + \Psi(x_-(x, \xi)))/4 \geq 1/4$. Therefore,

$$\forall f \in H_0^1(\Omega): \quad \| f \|_{H^1(\Omega)} \leq C_1 \left(\| \mathbf{W}_T^\sharp \mathbf{\Psi W}_{T,\Omega} f \|_{H^1(\Omega)} + \| f \|_{L^2(\Omega)} \right).$$

Because $\mathbf{W}_T^\sharp \mathbf{\Psi W}_{T,\Omega} f$ is supported inside $\Omega_{2T}^{(1)}$, we have

$$\begin{aligned} \| \mathbf{W}_T^\sharp \mathbf{\Psi W}_{T,\Omega} f \|_{H^1(\Omega)} &\leq \| \mathbf{W}_T^\sharp \mathbf{\Psi W}_{T,\Omega} f \|_{H^1(\Omega_{2T}^{(1)})} \\ &\leq C_2 \| \mathbf{W}_T^\sharp \mathbf{\Psi W}_{T,\Omega} f \|_{H_0^1(\Omega_{2T}^{(1)})} \\ &\leq C_3 \| \mathbf{\Psi W}_{T,\Omega} f \|_{H_0^1(\Omega_T^{(1)})}. \end{aligned}$$

Above, the last inequality comes from the conservation of the energy $\int_{\mathbb{R}^n} \left[c^{-2} |\partial_t q(\cdot, t)|^2 + |\nabla q(\cdot, t)|^2 \right] dx$ for (2.4) and $\partial_t q(\cdot, T) \equiv 0$. From the last two displayed equations we conclude

$$\forall f \in H_0^1(\Omega): \quad \| f \|_{H_0^1(\Omega)} \leq C_4 \left(\| \mathbf{W}_{T,\Omega} f \|_{H^1(\overline{\Omega}^c)} + \| f \|_{L^2(\Omega)} \right). \tag{2.8}$$

Since $\mathbf{W}_{T,\Omega}$ is injective, and the embedding $H_0^1(\Omega) \to L_2(\Omega): f \mapsto f$ is compact, applying [35, Proposition 5.3.1] to (2.8) concludes the proof. ■

Let us briefly discuss the condition that $T > T_0/2$ posed in Theorem 2.8. It implies for any $(x, \xi) \in T^*\Omega$, at least either $x_+(x, \xi) \coloneqq \gamma_{x,\xi}(T)$ or $x_-(x,\xi) \coloneqq \gamma_{x,\xi}(-T)$ belongs to Ω^c. That is, if $(x, \xi) \in \mathrm{WF}(f)$ then either $(x_+(x, \xi), \xi_+(x, \xi) \coloneqq \zeta_{x,\xi}(t)) \in \mathrm{WF}(\mathbf{W}_{T,\Omega} f)$ or $(x_-(x, \xi), \xi_-(x, \xi) \coloneqq \zeta_{x,-\xi}(t)) \in \mathrm{WF}(\mathbf{W}_{T,\Omega} f)$. We, hence, say that all the singularities of f are observed by $\mathbf{W}_{T,\Omega} f$. Therefore, $T > T_0/2$ is called the **visibility condition**. We will always assume it in our subsequent presentation.

3. Iterative time-reversal.

Consider the extension operator $\mathbf{E}_\Omega: H^1(\overline{\Omega}^c) \to H^1(\mathbb{R}^n)$ defined as follows. For any $g \in H^1(\overline{\Omega}^c)$, we take $\mathbf{E}_\Omega(g)|_{\Omega^c} = g$ on Ω^c and define $\mathbf{E}_\Omega(g)$ on Ω as the harmonic extension of g to Ω. That is, $h \coloneqq \mathbf{E}_\Omega(g)|_\Omega$ satisfies the Dirichlet problem:

$$\begin{cases} \Delta h = 0 & \text{in } \Omega \\ h = g|_{\partial\Omega} & \text{on } \partial\Omega . \end{cases} \tag{3.1}$$

Here, $g|_{\partial\Omega} \in H^{1/2}(\partial\Omega)$ denotes the trace of $g \in H^1(\overline{\Omega}^c)$ on $\partial\Omega$. Note that the Dirichlet interior problem (3.1) has a unique solution $h \in H^1(\Omega)$ (see, for example, [22]); therefore, noting that $\mathbf{E}_\Omega(g) = g$ on Ω^c, $\mathbf{E}_\Omega(g) \in H^1(\mathbb{R}^n)$. For notational conveniences, we sometimes use the short-hand notation $\bar{g}$ for $\mathbf{E}_\Omega(g)$. We further define the orthogonal projection $\mathbf{P}_\Omega: H^1(\Omega) \to H_0^1(\Omega): g \mapsto g - h$, where $h \in H^1(\Omega)$ is the solution of (3.1).

Recall that our aim is the inversion of the restricted single time wave inversion operator $\mathbf{W}_{T,\Omega}: H_0^1(\Omega) \to H^1(\overline{\Omega}^c)$ defined by (1.2). Our proposed inversion approach is based on the *modified time-reversal* operator defined by

$$\mathbf{W}_{T,\Omega}^\sharp \coloneqq \mathbf{P}_\Omega \mathbf{W}_T^\sharp \mathbf{E}_\Omega: H^1(\overline{\Omega}^c) \to H_0^1(\Omega) .$$

The modified time-reversal operator is itself the composition of harmonic extension $\mathbf{E}_\Omega$ to $\mathbb{R}^n$, time-reversal $\mathbf{W}_T^\sharp$ defined by (2.5) and projection $\mathbf{P}_\Omega$ onto $H_0^1(\Omega)$.

3.1. Contraction property.

Consider the case $n = 1$, the sound speed is constant, and $T > T_0$. Then, from the D'Alembert formula, $2\mathbf{W}_{T,\Omega}^\sharp$ is the exact inverse of $\mathbf{W}_{T,\Omega}$. In the general case this is not true. Nevertheless, as the basis our approach, we will show that the error operator $\mathrm{Id} - \lambda \mathbf{W}_{T,\Omega}^\sharp \mathbf{W}_{T,\Omega}$ is non-expansive for $\lambda = 2$ and a contraction for $\lambda < 2$. This will serve as the basis of the proposed iterative time-reversal procedure.

Throughout the following we denote by $E_u(t) \coloneqq \int_{\mathbb{R}^n} \left[c^{-2}(x) |\partial_t u(x,t)|^2 + |\nabla u(x,t)|^2 \right] \mathrm{d}x$ the energy associated to a function u satisfying the wave equation $\partial_t^2 u = c^2 \Delta u$.

Theorem 3.1 (Contraction property of the error operator). *Suppose* $T > T_0/2$ *and consider for any* $\lambda \in (0, 2]$ *the error operator*

$$\mathbf{K}_{T,\Omega,\lambda} := \mathrm{Id} - \lambda \mathbf{W}^{\sharp}_{T,\Omega}\mathbf{W}_{T,\Omega} : H^1_0(\Omega) \to H^1_0(\Omega).$$

Then the following hold:

- **a.** $\mathbf{K}_{T,\Omega,2}$ *satisfies* $\forall f \in H^1_0(\Omega) \setminus \{0\} : \|\mathbf{K}_{T,\Omega,2} f\|_{H^1_0(\Omega)} < \| f \|_{H^1_0(\Omega)}$.
- **b.** *If* $\lambda \in (0, 2)$, *then* $\|\mathbf{K}_{T,\Omega,\lambda}\| < 1$.

Proof. (a): For $f \in H^1_0(\Omega)$, set $g := \mathbf{W}_{T,\Omega} f$ and $\tilde{g} := \mathbf{W}_T f$. That is, $\tilde{g} = p(\cdot, T)$ and $g = \tilde{g}|_{\bar{\Omega}^c}$, where p solves the forward problem (1.1). Let $\bar{g} := \mathbf{E}_{\Omega}(g)$ and q solve the time-reversal problem (2.4) with $h = 2\bar{g}$. Then $w := p - q$ satisfies the wave equation $\partial_t^2 w = c^2 \Delta w$ and the corresponding energies at times 0 and T respectively satisfy

$$\begin{aligned} E_w(0) &= \int_{\mathbb{R}^n} \left[c^{-2}(x) |\partial_t q(x, 0)|^2 + \left| \nabla [q(x, 0) - f(x)] \right|^2 \right] \mathrm{d}x, \\ E_w(T) &= \int_{\mathbb{R}^n} \left[c^{-2}(x) |\partial_t p(x, T)|^2 + \left| \nabla [2\bar{g}(x) - \tilde{g}(x)] \right|^2 \right] \mathrm{d}x. \end{aligned} \tag{3.2}$$

Since $\bar{g}|_{\partial\Omega} = \tilde{g}|_{\partial\Omega}$ and $(\Delta \bar{g})|_{\Omega} = 0$,

$$\begin{aligned} &\int_{\Omega} |\nabla [2\bar{g}(x) - \tilde{g}(x)]|^2 - |\nabla \tilde{g}(x)|^2 \, \mathrm{d}x = 4 \int_{\Omega} \nabla \bar{g}(x) \cdot \nabla [\bar{g}(x) - \tilde{g}(x)] \mathrm{d}x \\ &= 4 \int_{\Omega} \Delta \bar{g}(x) [\bar{g}(x) - \tilde{g}(x)] \mathrm{d}x = 0. \end{aligned}$$

That is, $\int_{\Omega} |\nabla [2\bar{g}(x) - \tilde{g}(x)]|^2 \mathrm{d}x = \int_{\Omega} |\nabla \tilde{g}(x)|^2 \, \mathrm{d}x$. Noting that $\tilde{g} = \bar{g}$ on Ω^c, we obtain $\int_{\mathbb{R}^n} |\nabla [2\bar{g}(x) - \tilde{g}(x)]|^2 \, \mathrm{d}x = \int_{\mathbb{R}^n} |\nabla \tilde{g}(x)|^2 \, \mathrm{d}x$. From (3.2) we deduce $E_w(T) = E_p(T)$. With the conservation of energy we have $E_p(0) = E_w(0)$ and therefore

$$\int_{\mathbb{R}^n} \left| \nabla f(x) \right|^2 \mathrm{d}x = \int_{\mathbb{R}^n} \left[c^{-2}(x) |\partial_t q(x, 0)|^2 + \left| \nabla [q(x, 0) - f(x)] \right|^2 \right] \mathrm{d}x, \tag{3.3}$$

where we have used the explicit expressions for $E_p(0)$ and $E_w(0)$ respectively.

With $f^* := 2\mathbf{W}^{\sharp}_{T,\Omega}\mathbf{W}_{T,\Omega} f$ the error operator satisfies $\mathbf{K}_{T,\Omega,2} f = f - f^*$. Moreover, writing $q_0 := q(\cdot, 0)|_{\Omega}$ we have $f^* = \mathbf{P}_{\Omega}(q_0)$ and thus $\Delta[q_0 - f^*] = 0$ in Ω. From this we infer $\int_{\Omega} \nabla [q_0(x) - f^*(x)] \cdot \nabla [f^*(x) - f(x)] \, \mathrm{d}x = -\int_{\Omega} \Delta [q_0(x) - f^*(x)][f^*(x) - f(x)] \, \mathrm{d}x = 0$ and therefore

$$\begin{aligned} &\int_{\Omega} |\nabla [q_0(x) - f(x)]|^2 \, \mathrm{d}x = \int_{\Omega} |\nabla [q_0(x) - f^*(x)]|^2 \, \mathrm{d}x + \int_{\Omega} |\nabla [f^*(x) - f(x)]|^2 \, \mathrm{d}x \\ &\geq \int_{\Omega} |\nabla [f^*(x) - f(x)]|^2 \, \mathrm{d}x \\ &. \end{aligned} \tag{3.4}$$

Together with (3.3) this implies $\| f \|^2_{H^1_0(\Omega)} \geq \|f - f^*\|^2_{H^1_0(\Omega)}$. That is, $\|\mathbf{K}_{T,\Omega,2} f\|_{H^1_0(\Omega)} \leq \| f \|_{H^1_0(\Omega)}$.

In remains to show the strict inequality. To that end assume $\|f - f^*\|_{H^1_0(\Omega)} = \| f \|_{H^1_0(\Omega)}$. From (3.3) and (3.4) we obtain

$$\int_\Omega |\nabla [q_0(x) - f(x)]|^2 \mathrm{d}x \geq \int_{\mathbb{R}^n} \left[c^{-2}(x) |\partial_t q(x,0)|^2 + \left| \nabla [q(x,0) - f(x)] \right|^2 \right] \mathrm{d}x,$$

and therefore

$$\int_{\mathbb{R}^n} c^{-2}(x) |\partial_t q(x,0)|^2 \, \mathrm{d}x + \int_{\Omega^c} \left| \nabla q(x,0) \right|^2 \, \mathrm{d}x = 0.$$

In particular, $\partial_t q(\cdot,0)$ vanishes on $\mathbb{R}^n$ and $\nabla q(\cdot,0)$ vanishes on Ω^c. Because $q(x, 0)$ vanishes for $x \in \Omega^{(2)}_{2T}$, it follows that $q(\cdot,0)$ vanishes on Ω^c. Applying Lemma 2.1 for $u(\cdot,t) \coloneqq q(\cdot, T-t)$ yields $2\bar{g} = q(\cdot, T) = u(\cdot, 0) = 0$ on $\mathbb{R}^n$. In particular, $\mathbf{W}_{T,\Omega} f = 0$ on Ω^c. From Theorem 2.4, we infer $f = 0$ on $\mathbb{R}^n$, which concludes the proof.

(b): Let us first consider the case $\lambda = 1$. We have to show that there exists a constant $L < 1$ such that $\| \mathrm{Id} - \mathbf{W}^\sharp_{T,\Omega} \mathbf{W}_{T,\Omega} \| \leq L$. To that end, let $f \in H^1_0(\Omega)$, p solve the forward model (1.1) with initial data f, q solve the time-reversal problem (2.4) with initial data $h = \mathbf{E}_\Omega \mathbf{W}_{T,\Omega} f$ and define the error term $w \coloneqq q - p$. The error term satisfies the wave equation $\partial_t^2 w - c^2(x) \Delta w = 0$ in $\mathbb{R}^n \times (0, T)$ and its energy at time T is given by

$$\begin{aligned} E_w(T) &= \int_{\mathbb{R}^n} \left[c^{-2}(x) |\partial_t w(x,T)|^2 + \left| \nabla w(x,T) \right|^2 \right] \mathrm{d}x \\ &= \int_{\mathbb{R}^n} c^{-2}(x) |\partial_t p(x,T)|^2 \, \mathrm{d}x + \int_{\mathbb{R}^n} \left| \nabla [\bar{g}(x) - \tilde{g}(x)] \right|^2 \, \mathrm{d}x, \end{aligned}$$

where for the second equality we used the conditions $q(\cdot, T) = \bar{g}$ and $\partial_t g(\cdot, T) = 0$. The functions $\tilde{g}$ and $\bar{g}$ are defined as above, in the proof of (a).

The second term in the above equation displayed satisfies

$$\begin{aligned} &\int_{\mathbb{R}^n} \left| \nabla [\bar{g}(x) - \tilde{g}(x)] \right|^2 \, \mathrm{d}x = \\ &= \int_{\mathbb{R}^n} \nabla [\tilde{g}(x) - \bar{g}(x)] \cdot \nabla [\tilde{g}(x) - \bar{g}(x)] \, \mathrm{d}x \\ &= \int_{\mathbb{R}^n} \nabla [\tilde{g}(x) - \bar{g}(x)] \cdot \nabla [\tilde{g}(x) + \bar{g}(x)] \, \mathrm{d}x - 2 \int_{\mathbb{R}^n} \nabla [\tilde{g}(x) - \bar{g}(x)] \cdot \nabla \bar{g}(x) \, \mathrm{d}x \\ &= \int_\Omega \left| \nabla \tilde{g}(x) \right|^2 \, \mathrm{d}x - \int_\Omega \left| \nabla \bar{g}(x) \right|^2 \, \mathrm{d}x - 2 \int_{\mathbb{R}^n} (\tilde{g}(x) - \bar{g}(x)) \Delta \bar{g}(x) \, \mathrm{d}x \\ &= \int_\Omega \left| \nabla \tilde{g}(x) \right|^2 \, \mathrm{d}x - \int_\Omega \left| \nabla \bar{g}(x) \right|^2 \, \mathrm{d}x \\ &\leq \int_\Omega \left| \nabla \tilde{g}(x) \right|^2 \, \mathrm{d}x \,. \end{aligned}$$

As a consequence, recalling $g = \tilde{g}|_{\overline{\Omega}^c} = \mathbf{W}_{T,\Omega} f$, we obtain

$$E_w(T) \le \int_{\mathbb{R}^n}\left[c^{-2}(x)|\partial_t p(x,T)|^2 + \left|\nabla \tilde{g}(x)\right|^2\right]\mathrm{d}x - \int_{\Omega^c}\left|\nabla g(x)\right|^2\,\mathrm{d}x$$
$$= \int_{\mathbb{R}^n}\left[c^{-2}(x)|\partial_t p(x,T)|^2 + \left|\nabla p(x,T)\right|^2\right]\mathrm{d}x - \|\nabla \mathbf{W}_{T,\Omega} f\|^2_{L^2(\bar{\Omega}^c)}$$
$$= E_p(T) - \|\nabla \mathbf{W}_{T,\Omega} f\|^2_{L^2(\bar{\Omega}^c)}.$$

The conservation of energy for E and p then gives

$$E_w(0) + \|\nabla \mathbf{W}_{T,\Omega} f\|^2_{L^2(\bar{\Omega}^c)} = E_w(T) + \|\nabla \mathbf{W}_{T,\Omega} f\|^2_{L^2(\bar{\Omega}^c)}$$
$$\le E_p(T) = E_p(0).$$

Using the initial conditions $p(x, 0) = f(x)$ and $\partial_t p(x, 0) = 0$ this shows

$$E_w(0) + \|\nabla \mathbf{W}_{T,\Omega} f\|^2_{L^2(\bar{\Omega}^c)} \le \| f \|^2_{H^1_0(\Omega)}.$$

Noting that $\mathbf{W}_{T,\Omega} f$ vanishes outside of $\Omega_T^{(2)}$, we have $\|\nabla \mathbf{W}_{T,\Omega} f\|^2_{L^2(\bar{\Omega}^c)} \ge \mu \|\mathbf{W}_{T,\Omega} f\|^2_{H^1(\bar{\Omega}^c)}$, for some $\mu > 0$. Applying Theorem 2.8 we obtain

$$E_w(0) \le L^2 \| f \|^2_{H^1_0(\Omega)},$$

for some $0 < L < 1$. Noting that $E_w(0) = \int_{\mathbb{R}^n}\left[c^{-2}(x)|\partial_t q(x,0)|^2 + |\nabla[q(x,0) - f(x)]|^2\right]\mathrm{d}x$, we obtain

$$\int_\Omega \left|\nabla[q(x,0) - f(x)]\right|^2 \mathrm{d}x \le L^2 \| f \|^2_{H^1_0(\Omega)}. \tag{3.5}$$

Let $f^* := \mathbf{W}^\sharp_{T,\Omega}\mathbf{W}_{T,\Omega} f$ and $q_0 = q(\cdot,0)|_\Omega$, then $f^* = \mathbf{P}_\Omega(q_0)$. The left hand side in the above equation can be estimated as

$$\int_\Omega |\nabla[q_0(x) - f(x)]|^2\,\mathrm{d}x = \int_\Omega |\nabla[q_0(x) - f^*(x)] + \nabla[f^*(x) - f(x)]|^2\,\mathrm{d}x$$
$$= \int_\Omega |\nabla[q_0(x) - f^*(x)]|^2 + |\nabla[f^*(x) - f(x)]|^2\,\mathrm{d}x$$
$$\ge f^* - f^2_{H^1_0(\Omega)},$$

where we have used the fact that
$\int_\Omega \nabla[q_0(x) - f^*(x)] \cdot \nabla[f^*(x) - f(x)]\,\mathrm{d}x = \int_\Omega \Delta[q_0(x) - f^*(x)][f^*(x) - f(x)]\mathrm{d}x = 0$. From 3.5, we arrive at

$$\|\mathbf{K}_1 f\|^2_{H^1_0(\Omega)} = \|f - f^*\|^2_{H^1_0(\Omega)} \le L^2 \| f \|^2_{H^1_0(\Omega)}.$$

This finishes the proof for the case $\lambda = 1$.

For the general case note the identities

$$\mathbf{K}_{T,\Omega,\lambda} = \begin{cases} (1-\lambda)\,\mathrm{Id} + \lambda \mathbf{K}_{T,\Omega,1} & \text{for } \lambda \in (0,1) \\ (\lambda-1)\mathbf{K}_{T,\Omega,2} + (2-\lambda)\mathbf{K}_{T,\Omega,1} & \text{for } \lambda \in (1,2)\,. \end{cases}$$

Using the already verified estimates $\|\mathbf{K}_{T,\Omega,1}\| < 1$ and $\|\mathbf{K}_{T,\Omega,2}\| \leq 1$, these equalities together with the triangle inequality for the operator norm show $\|\mathbf{K}_{T,\Omega,\lambda}\| < 1$ for all $\lambda \in (0, 2)$. ■

3.2. Neumann series solution.

According to Theorem 3.1 the error operator satisfies $\left\|\mathrm{Id} - \lambda \mathbf{W}^{\sharp}_{T,\Omega}\mathbf{W}_{T,\Omega}\right\| < 1$ for any $\lambda \in (0, 2)$. The Neumann series $\sum_{j=0}^{\infty}\left(\mathrm{Id} - \lambda \mathbf{W}^{\sharp}_{T,\Omega}\mathbf{W}_{T,\Omega}\right)^{j}$, therefore, converges to $\left(\lambda \mathbf{W}^{\sharp}_{T,\Omega}\mathbf{W}_{T,\Omega}\right)^{-1}$ with respect to the operator norm $\|\cdot\|$ in $H^{1}_{0}(\Omega)$. This results in the inversion formula

$$f = \sum_{j=0}^{\infty}\left(\mathrm{Id} - \lambda \mathbf{W}^{\sharp}_{T,\Omega}\mathbf{W}_{T,\Omega}\right)^{j}\left(\lambda \mathbf{W}^{\sharp}_{T,\Omega} g\right) \quad \text{with } g = \mathbf{W}_{T,\Omega} f \tag{3.6}$$

valid for every initial data $f \in H^{1}_{0}(\Omega)$. Here $\mathbf{W}^{\sharp}_{T,\Omega} = \mathbf{P}_{\Omega}\mathbf{W}^{\sharp}_{T}\mathbf{E}_{\Omega}$ is the modified time-reversal operator formed by harmonic extension $\mathbf{E}_{\Omega}$ of the missing data, time-reversal $\mathbf{W}^{\sharp}_{T}$ defined by (2.4) and projection $\mathbf{P}_{\Omega}$ onto H^{1}_{0}. Inversion formula (3.6) is the Neumann series solution for the inverse problem of full-field PAT.

Remark 3.2 (Iterative time-reversal algorithm). The Neumann series in (3.6) is the limit of its partial sums $f_k := \sum_{k=0}^{j}\left(\mathrm{Id} - \lambda \mathbf{W}^{\sharp}_{T,\Omega}\mathbf{W}_{T,\Omega}\right)^{k}\left(\lambda \mathbf{W}^{\sharp}_{T,\Omega} g\right)$. These partial sums satisfy the recursion

$$\begin{cases} f_0 = \lambda \mathbf{W}^{\sharp}_{T,\Omega} g \\ f_j = f_{j-1} - \lambda \mathbf{W}^{\sharp}_{T,\Omega}\left(\mathbf{W}_{T,\Omega} f_{j-1} - g\right), \end{cases} \tag{3.7}$$

with $\mathbf{W}^{\sharp}_{T,\Omega} = \mathbf{P}_{\Omega}\mathbf{W}^{\sharp}_{T}\mathbf{E}_{\Omega}$. This is an iterative algorithm producing a sequence $(f_j)_{j \in \mathbb{N}}$ converging to $f = \mathbf{W}^{-1}_{T,\Omega} g$ in $H^{1}_{0}(\Omega)$. We call (3.7) iterative reversal algorithm for full field PAT. The form (3.7) will be used in the numerical solution. Because of the contraction property of the iteration $\left\|\mathrm{Id} - \lambda \mathbf{W}^{\sharp}_{T,\Omega}\mathbf{W}_{T,\Omega}\right\| < 1$ the iterative time-reversal reversal algorithm is linearly convergent.

We note that for standard PAT, the idea of using time-reversal was proposed in [9, 7] for the case of constant sound speed, and in [10, 15] for non-constant sound speed. The Neumann series solution was first proposed in [32] and further developed in [32, 33, 36, 14, 34, 25, 29, 18, 1]. Iterative reconstruction methods for variable sound speed based on an adjoint wave equation have been studied in [16, 5, 3, 11, 17]. Uniqueness and stability for standard PAT was studied in [39, 15, 32, 33, 23], just to name a few.

4. Numerical Simulations.

In this section, we present some of our numerical studies for the exterior single time wave transform. We consider the case of two spatial dimensions, and take $\Omega \subseteq \mathbb{R}^2$ as the unit disc. According to (3.6) any function $f \in H^{1}_{0}(\Omega)$ can be recovered from data $g = \mathbf{W}_{T,\Omega} f$ via the iterative time-reversal algorithm (3.7). The numerical realization is described in the

following subsection. The numerical simulations were performed for each of the three sound speed profiles shown in the top row of Figure 1 and additionally for the constant sound speed $c_{\mathrm{I}} = 1$. The sound speed profiles c_{III} and c_{IV} are adopted from [31] where c_{III} is shown to be trapping and c_{IV} to be non-trapping. For the used radially symmetric sound speed profile $c_{\mathrm{III}} = c(\|x\|)$ the Herglotz condition $\frac{d}{dr}(r/(c(r))) > 0$ is satisfied which implies that c_{III} is non-trapping. As phantom we used numerical approximations of one smooth and two piecewise constant functions which are visualized in the bottom row of Figure 1.

4.1 Numerical implementation.

In the numerical realization, any function $h: \mathbb{R}^2 \to \mathbb{R}$ is represented by a discrete vector $(h(x_i))_{i_1, i_2 = 0}^{N-1} \in \mathbb{R}^{N \times N}$, where

$$x_i = (-a, -a) + 2ia/N \quad \text{for} \quad i = (i_1, i_2) \in \{0, \ldots, N-1\}^2$$

are equidistant grid points in the square $[-a, a]^2$. The discrete domain $I \subseteq \{0, \ldots, N-1\}^2$ (where the discrete initial pressure is contained in) is defined as the set of all indices i with $x_i \in \Omega$ and we set $J := \{0, \ldots, N-1\}^2 \setminus I$. Following [12], we define the discrete boundary of I as the set of all elements $(i_1, i_2) \in J$ for which at least one of the discrete neighbors $(i_1 + 1, i_2), (i_1 - 1, i_2), (i_1, i_2 + 1), (i_1, i_2 - 1)$ is contained in I. The discrete version of the initial data $f \in H_0^1(\Omega)$ is then an image $\mathtt{f} \in \mathbb{R}^I$ and the discrete version of the data $g \in L^2(\overline{\Omega}^c)$ an image $g \in \mathbb{R}^J$.

In the iterative time-reversal algorithm the forward transform $\mathbf{W}_{T,\Omega}$ as well as each factor in the modified time-reversal $\mathbf{W}_{T,\Omega}^{\sharp} = \mathbf{P}_{\Omega}\mathbf{W}_T^{\sharp}\mathbf{E}_{\Omega}$ are replaced by discrete approximations. The discrete forward operator and the discrete time-reversal operator are defined by

$$\mathtt{W}_{T,I}: \mathbb{R}^I \to \mathbb{R}^J : \mathtt{f} \mapsto (\mathtt{W}_T \mathtt{f})_{I^c} \tag{4.1}$$

$$\mathtt{W}_{T,I}^{\sharp}: \mathbb{R}^J \to \mathbb{R}^I : \mathtt{g} \mapsto \left(\mathtt{P}_I \mathtt{W}_T^{\sharp} \mathtt{E}_I\right)\mathtt{g}\,. \tag{4.2}$$

Here $\mathtt{W}_T: \mathbb{R}^{N \times N} \to \mathbb{R}^{N \times N}$ and $\mathtt{W}_T^{\sharp}: \mathbb{R}^{N \times N} \to \mathbb{R}^{N \times N}$ are discrete analogs of the forward wave equation and its time reversed version, $\mathtt{E}_I$ a discretization of the harmonic extension operator and $\mathtt{P}_I$ a discretization of the projection of the projection onto $H_0^1(\Omega)$.

The numerical solution of the wave equation $\mathtt{W}_T \mathtt{f}$ and likewise the numerical solution of the time reversed version $\mathtt{W}_T^{\#}$ are computed with the k-space method [6, 8, 21]. We use the k-space method with periodic boundary conditions on the rectangle $[-a, a]^2$ as described in [11]. We choose $a \geq T + 1$ such that $\mathtt{W}_{T,I}$ and $\mathtt{W}_{T,I}^{\#}$ are not affected by replacing the free space wave equation with its $(2a)$-periodic counterpart. The discrete harmonic extension $\mathtt{E}_I$ and the discrete projection $\mathtt{P}_I$ are constructed by numerically solving (3.1) with the MATLAB-routine solvepde.

4.2 Numerical results.

We first present results for data $g = W_T f$ without added noise. Figure 2 shows results with constant speed with relaxation parameter $\lambda = 2$ and 80 iterations. For smaller values of λ slightly better reconstructions have been obtained but required a slightly larger number of iterations. Figure 3 visualizes the pointwise error map $f^a - f^a_{\text{rec}}$ for the non-constant sound speed profiles using $\lambda = 1/2$ and $T = 2$. We see that accurate results are obtained for all sound speed profiles. The best results were obtained for the sound speed profile c_{II}, and the error functions do not contain any visible information of the original phantom. Because all reconstructions look equally well and very similar to the original phantom f^a, we did not show them here. Additional simulations with other smooth and non-smooth phantoms indicate that smooth phantoms generally result in better reconstructions than non-smooth ones.

Next, in Figure 4, we present results for noisy data where $W_T^\sharp f$ has been contaminated with normally distributed noise with a standard deviation δ of two percent of the maximal pressure value. In order to avoid inverse crime, data are simulated using a three times finer discretization than used for the reconstruction. We observe that in all cases the iteration process is stable when λ is chosen sufficiently small, i.e. $0 < \lambda \leq 1/2$, and the use of a stopping rule is not necessary. Moreover, the reconstructions are more accurate for smooth phantoms than for piecewise constant phantoms. Finally in Figure 5 we show results for the trapping sound speed c_{IV}. Also in this case, the iterative time-reversal works well for all phantoms even though the theory developed in the previous Sections does not fully apply in this situation.

5. Conclusion.

In this work we studied an inverse source problem appearing in full field PAT. Image reconstruction amounts to the inversion of the exterior final time wave transform $\mathbf{W}_{T,\Omega}$ that maps the initial data f supported in Ω to the solution of the wave equation at fixed time T restricted to the complement $\overline{\Omega}^c$. For non-constant sound speed, besides the work [13], to the best of our knowledge, inversion of $\mathbf{W}_{T,\Omega}$ is studied for the first time. We, for the first time, derived uniqueness and stability results. Moreover we showed convergence of the proposed iterative time-reversal reconstruction algorithm. For that purpose we have proven that $\mathrm{Id} - \lambda \mathbf{W}^\sharp_{T,\Omega} \mathbf{W}_{T,\Omega}$ is a contraction on $H^1_0(\Omega)$ for all $\lambda \in (0, 2)$ where $\mathbf{W}^\sharp_{T,\Omega}$ is a modified time-reversal operator. We also derived a numerical realization of the iterative time-reversal algorithm. Numerical results show accurate reconstruction for all sound speed profiles and all initial data.

Acknowledgments.

The authors would like to thank the anonymous referees for the helpful comments and suggestions. M.H. acknowledges support of the Austrian Science Fund (FWF), project P 30747-N32. The research of L.N. has been supported by the National Science Foundation (NSF) Grants DMS 1212125 and DMS 1616904. L.N.'s research reported in this publication was also supported by the National Institute Of General Medical Sciences of the National Institutes of Health under Award Number P20GM104420. The content is solely the responsibility of the authors and does not necessarily represent the official views of the National Institutes of Health.

REFERENCES

[1]. Acosta S and Palacios B, Thermoacoustic tomography for an integro-differential wave equation modeling attenuation, Journal of Differential Equations, 264 (2018), pp. 1984–2010.

[2]. Agranovsky M and Kuchment P, The support theorem for the single radius spherical mean transform, Memoirs on Differential Equations and Mathematical Physics, 52 (2011), pp. 1–16.

[3]. Arridge SR, Betcke MM, Cox BT, Lucka F, and Treeby BE, On the adjoint operator in photoacoustic tomography, Inverse Problems, 32 (2016), p. 115012.

[4]. Beard P, Biomedical photoacoustic imaging, Interface focus, 1 (2011), pp. 602–631. [PubMed: 22866233]

[5]. Belhachmi Z, Glatz T, and Scherzer O, A direct method for photoacoustic tomography with inhomogeneous sound speed, Inverse Problems, 32 (2016), p. 045005.

[6]. Bojarski NN, The k-space formulation of the scattering problem in the time domain, The Journal of the Acoustical Society of America, 72 (1982), pp. 570–584.

[7]. Burgholzer P, Matt GJ, Haltmeier M, and Paltauf G, Exact and approximative imaging methods for photoacoustic tomography using an arbitrary detection surface, Physical Review E, 75 (2007), p. 046706.

[8]. Cox B, Kara S, Arridge S, and Beard P, k-space propagation models for acoustically heterogeneous media: Application to biomedical photoacoustics, The Journal of the Acoustical Society of America, 121 (2007), pp. 3453–3464. [PubMed: 17552697]

[9]. Finch D and Patch SK, Determining a function from its mean values over a family of spheres, SIAM journal on mathematical analysis, 35 (2004), pp. 1213–1240.

[10]. Grün H, Nuster R, Paltauf G, Haltmeier M, and Burgholzer P, Photoacoustic tomography of heterogeneous media using a model-based time reversal method, in Photons Plus Ultrasound: Imaging and Sensing 2008: The Ninth Conference on Biomedical Thermoacoustics, Optoacoustics, and Acousto-optics, vol. 6856, International Society for Optics and Photonics, 2008, p. 685620.

[11]. Haltmeier M and Nguyen LV, Analysis of iterative methods in photoacoustic tomography with variable sound speed, SIAM Journal on Imaging Sciences, 10 (2017), pp. 751–781.

[12]. Haltmeier M and Nguyen LV, Analysis of iterative methods in photoacoustic tomography with variable sound speed, SIAM J. Imaging Sci, 10 (2017), pp. 751–781, 10.1137/16M1104822.

[13]. Haltmeier M, Zangerl G, Nguyen LV, and Nuster R, Photoacoustic image reconstruction from full field data in heterogeneous media, in Photons Plus Ultrasound: Imaging and Sensing 2019, vol. 10878, International Society for Optics and Photonics, 2019, p. 108783D.

[14]. Homan A, Multi-wave imaging in attenuating media, Inverse Problems & Imaging, 7 (2013), p. 1235.

[15]. Hristova Y, Kuchment P, and Nguyen L, Reconstruction and time reversal in thermoacoustic tomography in acoustically homogeneous and inhomogeneous media, Inverse problems, 24 (2008), p. 055006.

[16]. Huang C, Wang K, Nie L, Wang LV, and Anastasio MA, Full-wave iterative image reconstruction in photoacoustic tomography with acoustically inhomogeneous media, IEEE transactions on medical imaging, 32 (2013), pp. 1097–1110. [PubMed: 23529196]

[17]. Javaherian A and Holman S, A continuous adjoint for photo-acoustic tomography of the brain, Inverse Problems, 34 (2018), p. 085003.

[18]. Katsnelson V and Nguyen LV, On the convergence of the time reversal method for thermoacoustic tomography in elastic media, Applied Mathematics Letters, 77 (2018), pp. 79–86.

[19]. Kuchment P, The Radon transform and medical imaging, SIAM, 2013.

[20]. Kuchment P and Kunyansky L, Mathematics of thermoacoustic tomography, European Journal of Applied Mathematics, 19 (2008), pp. 191–224.

[21]. Mast TD, Souriau LP, Liu DD, Tabei M, Nachman AI, and Waag RC, A k-space method for large-scale models of wave propagation in tissue, IEEE Transactions on Ultrasonics, Ferroelectrics, and Frequency Control, 48 (2001), pp. 341–354. [PubMed: 11370348]

[22]. McLean W and McLean WCH, Strongly elliptic systems and boundary integral equations, Cambridge university press, 2000.

[23]. Nguyen LV, On singularities and instability of reconstruction in thermoacoustic tomography, Tomography and inverse transport theory, Contemporary Mathematics, 559 (2011), pp. 163–170.

[24]. Nguyen LV, Spherical mean transform: a pde approach, Inverse Problems & Imaging, 7 (2013), p. 243.

[25]. Nguyen LV and Kunyansky LA, A dissipative time reversal technique for photoacoustic tomography in a cavity, SIAM Journal on Imaging Sciences, 9 (2016), pp. 748–769.

[26]. Nuster R, Slezak P, and Paltauf G, High resolution three-dimensional photoacoustic tomography with CCD-camera based ultrasound detection, Biomedical optics express, 5 (2014), pp. 2635–2647. [PubMed: 25136491]

[27]. Nuster R, Zangerl G, Haltmeier M, and Paltauf G, Full field detection in photoacoustic tomography, Optics Express, 18 (2010), pp. 6288–6299. [PubMed: 20389652]

[28]. Oraevsky AA, Jacques SL, and Esenaliev RO, Optoacoustic imaging for medical diagnosis, 1998. US Patent 5,840,023.

[29]. Palacios B, Reconstruction for multi-wave imaging in attenuating media with large damping coefficient, Inverse Problems, 32 (2016), p. 125008.

[30]. Poudel J, Lou Y, and Anastasio MA, A survey of computational frameworks for solving the acoustic inverse problem in three-dimensional photoacoustic computed tomography, Physics in Medicine & Biology, 64 (2019), p. 14TR01.

[31]. Qian J, Stefanov P, Uhlmann G, and Zhao H, An efficient neumann series–based algorithm for thermoacoustic and photoacoustic tomography with variable sound speed, SIAM Journal on Imaging Sciences, 4 (2011), pp. 850–883.

[32]. Stefanov P and Uhlmann G, Thermoacoustic tomography with variable sound speed, Inverse Problems, 25 (2009), p. 075011.

[33]. Stefanov P and Uhlmann G, Thermoacoustic tomography arising in brain imaging, Inverse Problems, 27 (2011), p. 045004.

[34]. Stefanov P and Yang Y, Multiwave tomography in a closed domain: averaged sharp time reversal, Inverse Problems, 31 (2015), p. 065007.

[35]. Taylor ME, Partial differential equations. 1, Basic theory, Springer, 1996.

[36]. Tittelfitz J, Thermoacoustic tomography in elastic media, Inverse Problems, 28 (2012), p. 055004.

[37]. Trèves F, Introduction to pseudodifferential and Fourier integral operators Volume 2: Fourier integral operators, vol. 2, Springer Science & Business Media, 1980.

[38]. Xu M and Wang LV, Photoacoustic imaging in biomedicine, Review of scientific instruments, 77 (2006), p. 041101.

[39]. Xu Y, Wang LV, Ambartsoumian G, and Kuchment P, Reconstructions in limited-view thermoacoustic tomography, Medical physics, 31 (2004), pp. 724–733. [PubMed: 15124989]

[40]. Zangerl G, Haltmeier M, Nguyen LV, and Nuster R, Full field inversion in photoacoustic tomography with variable sound speed, Applied Sciences, 9 (2019), p. 1563.

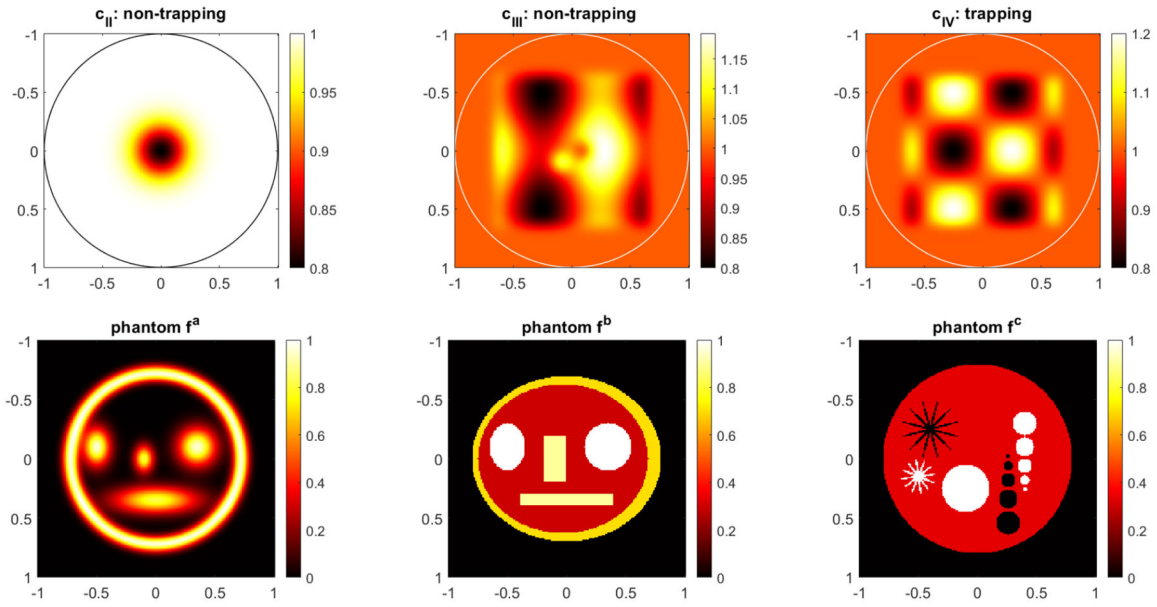

Figure 1. Sound speeds profiles and initial pressure distributions.

Top: Three non-trapping (c_{II} and c_{III}) and one trapping sound speed profile c_{IV} that we employed in our simulations besides the constant speed of sound $c_I = 1$. The white and black circles visualize the boundary of the imaging region which in our simulations is the unit disc. Bottom: A smooth phantom f^a (left) and the two piecewise constant phantoms f^b (middle) and f^c (right) are employed in our numerical simulations.

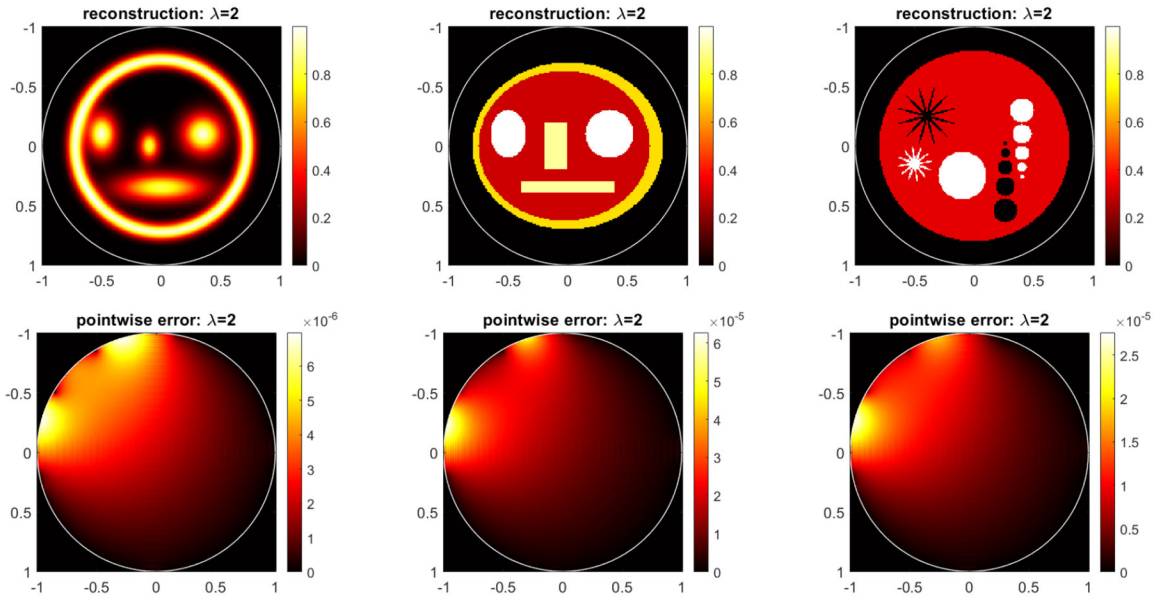

Figure 2. Results for constant sound speed.

Reconstructions (top) and corresponding point-wise errors (bottom) using constant sound speed $c_I = 1$.

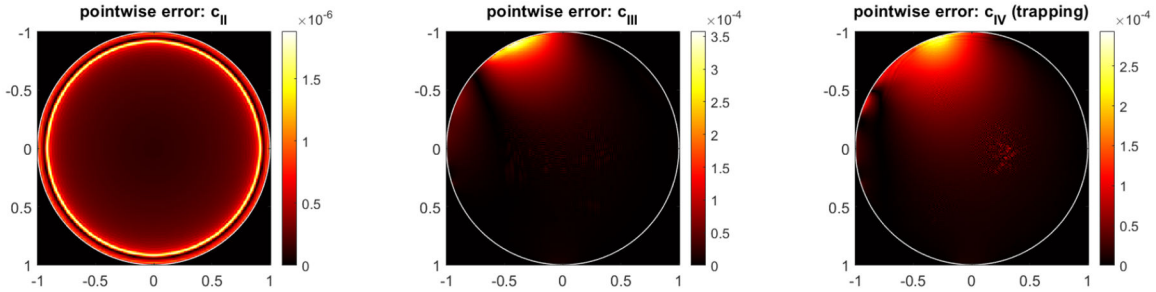

Figure 3. Results for variable sound speed.

Point-wise errors (bottom) using different sound speed profiles and the smooth phantom f[a].

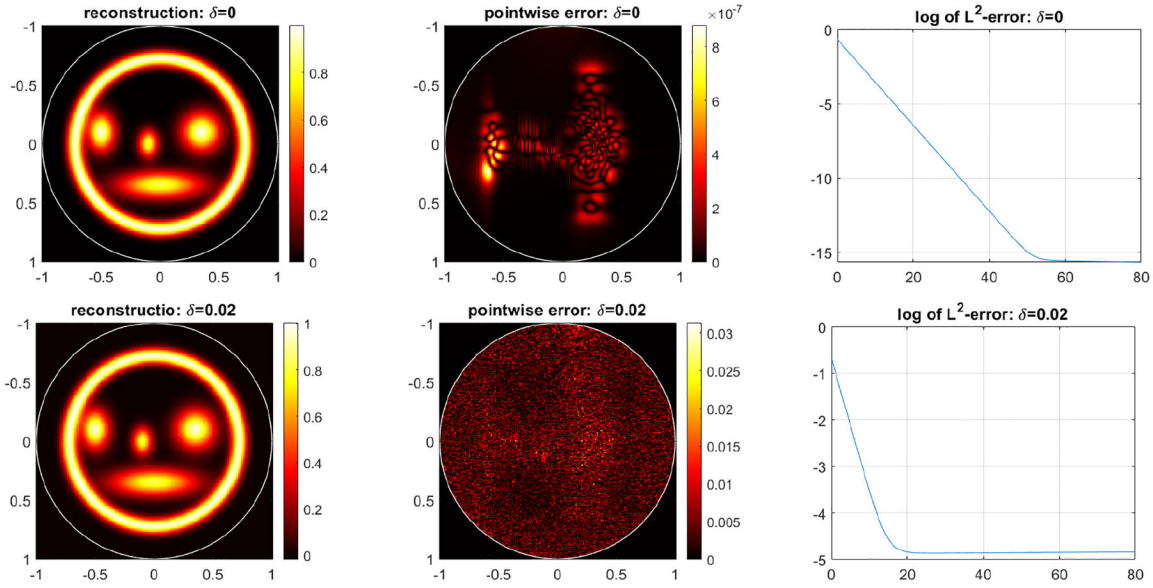

Figure 4. Exact versus noisy data for sound speed c_{III}.

From left to right: reconstruction, difference images to true phantom f^a, and logarithmic error plot in dependence of the number of iterations. The top row shows results for exact data, the bottom row shows results for noisy data with standard deviation $\delta = 0.02$. Here $\lambda = 1/2$ and $T = 4$. In this example, the observation time is twice as large as for the example in Fig 3, i.e. we have more data. This leads to a much smaller pointwise error for zero noise.

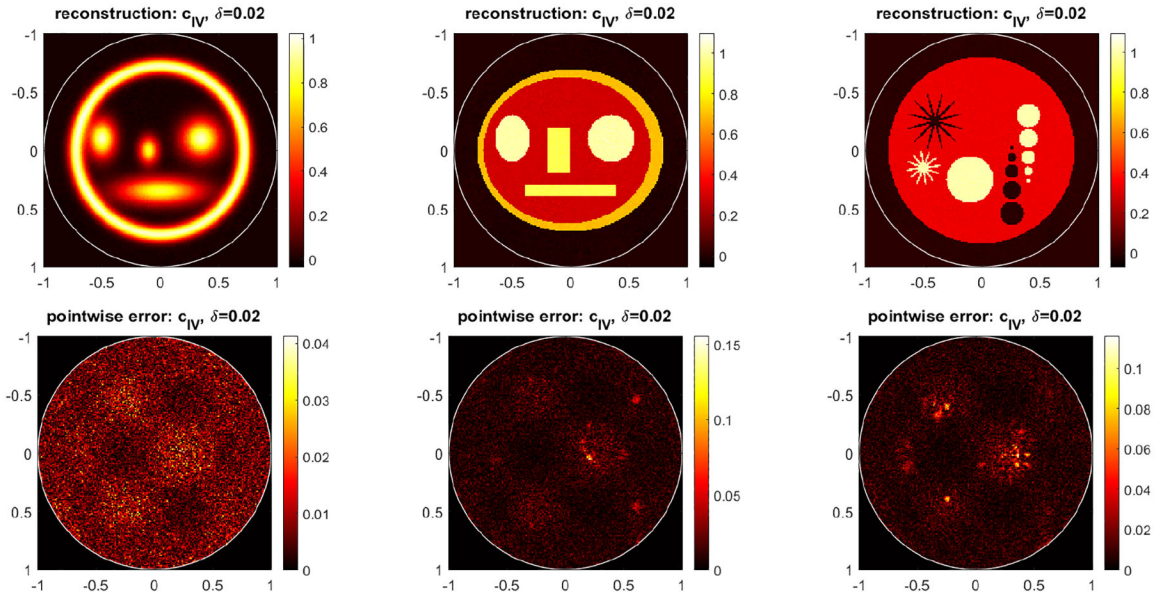

Figure 5. Results for noisy data for trapping sound speed c_{IV}.

Top row shows the reconstructions of the phantom f^a, f^b and f^c. Bottom row: Corresponding difference images for to the true phantom. Here $\lambda = 1/2$ and $T = 2$